Tellus
SERIES A
DYNAMIC
METEOROLOGY
AND OCEANOGRAPHY
PUBLISHED BY THE INTERNATIONAL METEOROLOGICAL INSTITUTE IN STOCKHOLM

Tellus (2009), 61A, 288–295
Printed in Singapore. All rights reserved

TELLUS

Doppler radar radial winds in HIRLAM. Part II: optimizing the super-observation processing

By K. SALONEN[1]*, H. JÄRVINEN[1], G. HAASE[2], S. NIEMELÄ[1] and R. ERESMAA[1], [1]*Finnish Meteorological Institute, P.O. Box 503, FI-00101, Helsinki, Finland;* [2]*Swedish Meteorological and Hydrological Institute, Norrköping, Sweden*

(Manuscript received 5 November 2007; in final form 5 November 2008)

ABSTRACT

Doppler radar radial wind observations are modelled in numerical weather prediction (NWP) within observation errors which consist of instrumental, modelling and representativeness errors. The systematic and random modelling errors can be reduced through a careful design of the observation operator (Part I). The impact of the random instrumental and representativeness errors can be decreased by optimizing the processing of the so-called super-observations (spatial averages of raw measurements; Part II).

The super-observation processing is experimentally optimized in this article by determining the optimal resolution for the super-observations for different NWP model resolutions. A 1-month experiment with the HIRLAM data assimilation and forecasting system is used for radial wind data monitoring and for generating observation minus background (OmB) differences. The OmB statistics indicate that the super-observation processing reduces the standard deviation of the radial wind speed OmB difference, while the mean vector wind OmB difference tends to increase. The optimal parameter settings correspond at a measurement range of 50 km (100 km) to an averaging area of 1.7 km^2 (7.3 km^2).

In conclusion, an accurate and computationally feasible observation operator for the Doppler radar radial wind observations is developed (Part I) and a super-observation processing system is optimized (Part II).

1. Introduction

In numerical weather prediction (NWP), observations are used to bring the NWP model state into the vicinity of the observed atmospheric state by using data assimilation techniques (e.g. Daley, 1991). Observation modelling makes use of the model variables and enables comparison of the model state with the observations. Generally, the observation model, usually called an observation operator, expresses the observed quantities in terms of the model variables. The observation operator is accurate within observation errors, which consist of instrumental, modelling and representativeness errors (Lorenc, 1986; Kalnay, 2003). Instrumental errors are due to random fluctuations of the instrument or data processing. Modelling errors are caused by deficiencies in the observation operator design. Representativeness errors are due to atmospheric phenomena which are detected by the observations but are not represented in the NWP model data due to its finite discretization (Liu and Rabier, 2003). These error sources consist of systematic and random contributions. Part I of this article focuses mainly on the systematic errors while the focus of Part II is on the random errors.

Usually in data assimilation, the observed quantity and its model counterpart are in a one-to-one correspondence: a model counterpart is computed for each observation. Abundance of some observation types, such as remote sensing measurements, allows attempts to average out random observation errors. By computing a spatial mean from a small number of measurements, a so-called super-observation (hereafter SO), random errors partly cancel out (Lorenc, 1981). This method has been in use, for instance, in the 1980s in the optimum interpolation analysis system (Lönnberg and Shaw, 1983) of the European Centre for Medium-Range Weather Forecast (ECMWF) to analyse the overly dense Western European synoptic surface network. More recently, SO processing methods have widely been used for remote sensing observations, such as atmospheric motion vectors (Berger et al., 2004), satellite soundings of temperature and moisture (Hart et al., 1993) and Doppler radar radial wind measurements (e.g. Albers, 1995; Seko et al., 2004).

Optimization of the SO processing from dense raw data is a trade-off between two factors regarding the spatial averaging. First, a small averaging area ensures that observations essentially represent the same atmospheric phenomena but it may be

*Corresponding author.
e-mail: kirsti.salonen@fmi.fi
DOI: 10.1111/j.1600-0870.2008.00381.x

insufficient in reducing random observation errors. Second, a large averaging area would result in a small random observation error, but different atmospheric phenomena may be represented if the observations used in the SO processing are too far apart. Thus, optimization of the SO processing is largely a question of deciding upon the size of the area that is used in the spatial averaging. Additionally, the resolution of the forecast model used in data assimilation sets its own requirements.

Characteristic for Doppler radars is that the measurement resolution is high compared with a typical NWP model resolution. Thus, the SO processing is definitely a viable option for the Doppler radar data. A Doppler radar is an azimuthally scanning instrument and the measured quantity is the radial wind component (towards or away from the radar antenna). For measurements of near-horizontal radial wind component, Doppler radars operate at very low elevation angles. In this context, a small averaging area implies a narrow sector in the azimuth direction and a short distance in the radial direction. Clearly, radial wind components vary with the azimuth angle. In the radial direction, varying range implies different measurement heights (for an elevation angle of 0.5°, a variation of some 90 m for each 10 km in range).

Doppler radar radial wind data and their error characteristics are studied in Part I of this article. Here, the focus is on random observation errors of the radial winds. The viewpoint is that the impact of the random instrumental errors can be minimized by optimizing the SO processing. The impact of the random representativeness errors may also be decreased to some extent as SOs may better represent the scales of the NWP model, and as spatial averaging has a smoothing effect on the observation errors. The impact of the random modelling errors is, however, thought to be beyond the capabilities of the SO processing.

In this article, the optimal resolution for the SOs is experimentally determined for varying NWP model resolutions. Experiments are performed with three different NWP model horizontal resolutions and eight SO resolutions, including radially thinned raw measurements. The article is organized as follows. Section 2 discusses the radar radial wind SO processing method of the High Resolution Limited Area Model (HIRLAM; Undén et al., 2002) NWP system. Section 3 describes the data sets and Section 4 presents the results from the model experiments, followed by a summary in Section 5.

2. Radar radial wind super-observations

2.1. The HIRLAM approach

Various methods to the radar radial wind SO processing have been discussed in the literature (e.g. Albers, 1995; Xiao et al., 2003; Seko et al., 2004; Swarbrick, 2006). The HIRLAM approach to the SO processing is based on horizontal averaging in polar space (Lindskog et al., 2000, 2004) and it is illustrated in Fig. 1. The desired SO resolution is defined with two free parameters, range bin spacing ($\overline{R}$) and azimuthal averaging ($\overline{\phi}$). Near the radar, raw observations used in the averaging are selected from a circle area limited by the arc distance of two adjacent output azimuth gates. At longer ranges where the arc distance exceeds $\overline{R}$, the data selection area is defined by $\overline{R}$. With this approach, fewer raw observations influence an SO near the radar than at longer measurement ranges. Each raw observation is restricted to influence only one SO.

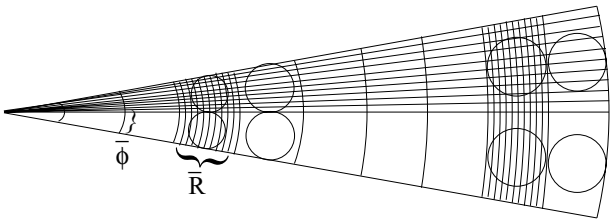

Fig. 1. Schematic illustration of SO processing. $\overline{R}$ is the range bin spacing and $\overline{\phi}$ is the azimuthal averaging.

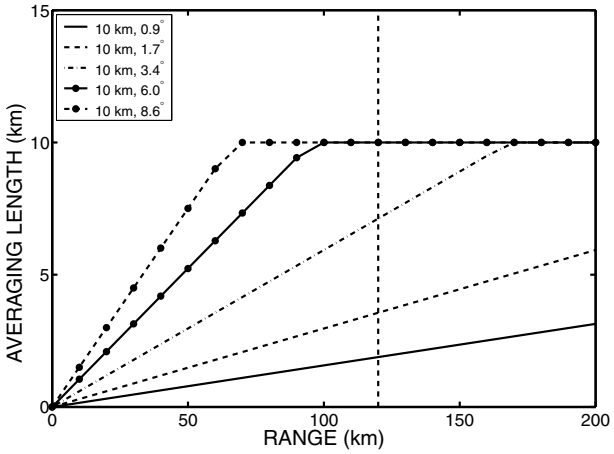

Fig. 2. Illustration of averaging lengths used in SO processing at different measurement ranges. Vertical dashed line indicates the maximum unambiguous measurement range of 120 km.

Typically, the maximum unambiguous measurement range of an operational C-band Doppler radar (operates on a wavelength of 4–8 cm and a frequency of 4–8 GHz) is 100–250 km. In practice, this means that the SO processing is dominated by $\overline{\phi}$. This is illustrated in Fig. 2, which shows the averaging area diameter, i.e. the averaging length, as a function of measurement range for different values of $\overline{\phi}$, when $\overline{R}$ is fixed to 10 km. For small values of $\overline{\phi}$, the range where the SOs reach their maximum averaging length is longer than the maximum unambiguous measurement range. For instance, for radars with a maximum unambiguous measurement range of 120 km (marked with vertical dashed line in Fig. 2), only SOs processed with values of 6.0° and 8.6° for $\overline{\phi}$ reach $\overline{R}$ within the range. Even though in most cases, $\overline{\phi}$ dominates the data averaging area, $\overline{R}$ defines the range spacing of the

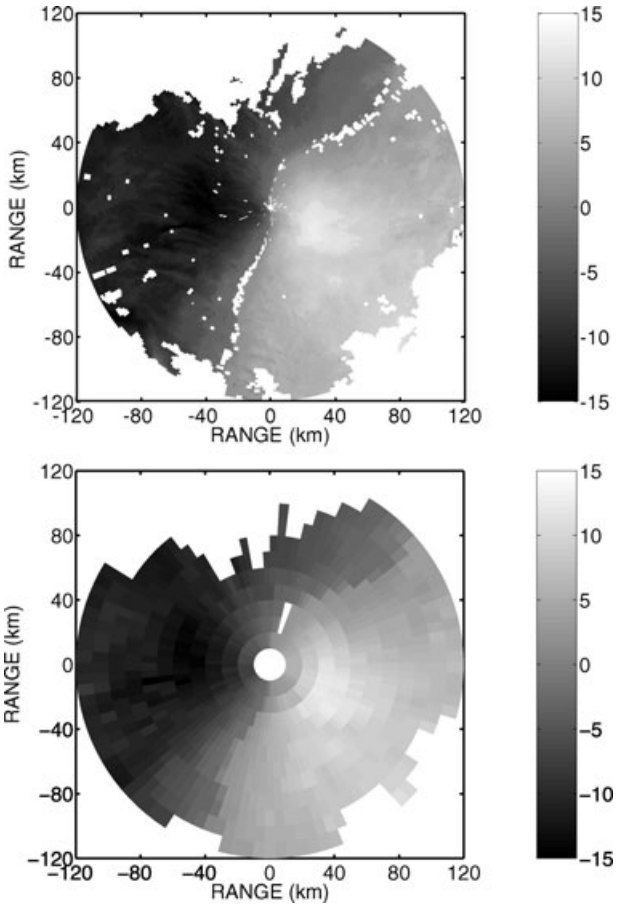

Fig. 3. Raw radar radial wind data (upper panel) and corresponding SOs generated with range bin spacing of 10 km, and azimuthal averaging of 3.4° (lower panel) at Karlskrona, 31 January 2002, 12 UTC.

SOs. Thus, the parameter $\overline{R}$ has a thinning effect in the radial direction.

An example of the SO processing is shown in Fig. 3. The upper panel of Fig. 3 shows raw radial wind observations from the radar at Karlskrona, Sweden, (56.30°N, 15.61°E) on 31 January 2002, 12 UTC. The lower panel shows the corresponding SOs processed with $\overline{R} = 10$ km and $\overline{\phi} = 3.4°$. Between azimuth angles of 40° (north-east) and 200° (southwest), the radar radial winds are mainly positive (away from the radar antenna) while elsewhere the radial winds are mainly negative (towards the radar antenna). Some local discontinuities can be seen in the raw observations. The lack of observations close to the zero Doppler velocity is because of the Doppler filtering, which is applied to reduce the effects of ground clutter. After horizontal averaging, the observed wind field is smoother (Fig. 3 lower panel) and local discontinuities have disappeared. Spatial averaging also fills in data sparse gaps.

2.2. *Artificial bias*

Averaging radial wind observations in the azimuthal direction is a potential source of artificial SO bias, as will be shown in the following. This is by no means specific to the HIRLAM method of SO processing but, in fact, a general feature of all SO processing methods applying azimuthal averaging.

The radial wind component has a cosine form as a function of azimuth angle in case of a uniform wind field. Intuitively, it is evident that averaging over azimuth angles reduces the maximum wind speeds towards and away from the radar antenna. Next, averaging as a potential source of artificial SO bias is illustrated with conceptual examples using a uniform and a linear wind field.

First, consider a uniform wind field and a 1° azimuthal resolution of the radar measurements. Figure 4 shows the maximum difference in per cent between the 'true' and the azimuthally averaged radial wind with gradually increasing averaging in the azimuthal direction. Averaging over three adjacent azimuth angles introduces in maximum a 0.01% artificial SO bias. Averaging over 15 azimuth angles introduces in maximum a 0.3% bias. This implies a 0.1 ms^{-1} maximum difference in case of a 40 ms^{-1} wind. It is still smaller than a typical accuracy of the radial wind measurement, which is of the order of 0.5 ms^{-1} (Holleman and Beekhuis, 2003). In case of a uniform wind field, the maximum artificial SO bias is present in 0.6% of the SOs while for the rest of the SOs the bias is smaller.

Second, the same analysis is repeated for a linear wind field which has a horizontal gradient of 15 ms^{-1} per 100 km. Also in this case, the largest differences occur at the maximum wind speeds towards and away from the radar antenna. The maximum SO bias is very similar as in case of a uniform wind field (not shown).

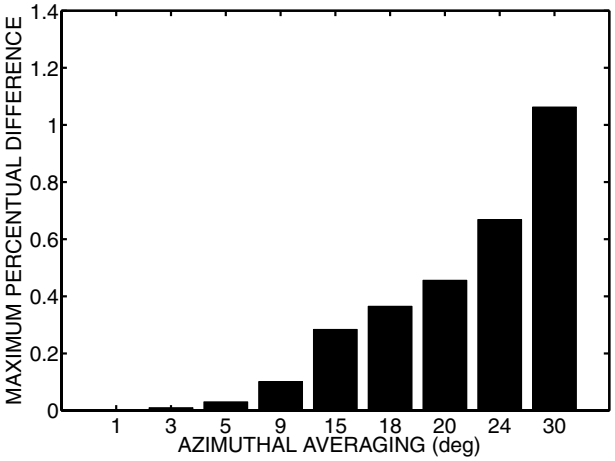

Fig. 4. Maximum percentual difference between the 'true' wind speed and the azimuthally averaged wind speed as a function of averaging angle.

Finally, the analysis is repeated for a uniform wind field of 40 ms^{-1} with one zero velocity value at the azimuth angle corresponding to the maximum wind speed to mimic a ground clutter observation. In this case, averaging over three (15) azimuth angles introduces a maximum difference of 0.6% (0.8%) to the averaged radial wind speed. Thus, the maximum differences are significantly larger than in the pure uniform wind field case due to the non-meteorological observation.

These examples demonstrate that averaging of the radial wind observations in the azimuthal direction introduces an artificial SO bias but convince that it is negligible at least when non-meteorological observations are not present in the data. In practical applications, averaging is typically done over a few azimuth gates and in these cases, the artificial SO bias is clearly negligible. The third example emphasizes the importance of proper clutter removal prior to the SO generation.

3. Experimental design

The HIRLAM SO processing is optimized as follows. Several SO data sets are processed with varying $\overline{R}$ and $\overline{\phi}$. Additionally, a subset of the original raw radial wind data set is made which is thinned in the radial direction. The data sets are passively monitored (not assimilated) using the HIRLAM data assimilation and forecasting system with different NWP model horizontal resolutions. The fit of the processed observations to the modelled radial winds is studied using statistics of the observation minus background (OmB) values. The aim of the experiments is to define the optimal combination of the SO processing parameters for different NWP model resolutions. Details of the observation data sets and HIRLAM model configurations are given next.

3.1. Observations

The raw radial wind measurements are from the radar at Karlskrona, Sweden (56.30°N, 15.61°E) for January 2002. The measurements are made with a dual-pulse repetition frequency (PRF) technique (Dazhang et al., 1984) at four to three ratio (1200 s^{-1}/ 900 s^{-1}). The maximum measurement range is 120 km, and the unambiguous velocity interval is ±48 ms^{-1}. Elevation angles of 0.5°, 1.1°, 2.3° and 3.2° are included in the data set. The resolution of the raw data is 1 km in range and 0.9° in azimuth (420 azimuth gates per 360° scan). Radar scans at different azimuth angles do not overlap as the radar pulse main lobe width is 0.9°. Observations are available every 15 min but in this study only observations made closest to the analysis time (00, 06, 12 and 18 UTC) are utilized and the rest of data are not used. The raw data set consists of 913 000 observations.

Table 1 summarizes the SO processing parameters. Two parameter sets are used. In the first set, $\overline{R}$ equals to 5–20 km while $\overline{\phi}$ is kept fixed at 1.7°. In the second set, $\overline{\phi}$ equals to 0.9°, 1.7°, 3.4°, 6.0° and 8.6°, respectively, while $\overline{R}$ is kept fixed at 10 km. The number of SOs in different data sets varies from 270 000 ($\overline{R}$ = 5 km and $\overline{\phi}$ = 1.7°) to 33 000 ($\overline{R}$ = 10 km and $\overline{\phi}$ = 8.6°). For $\overline{\phi}$ values of 0.9°, 1.7° and 3.4°, the maximum averaging lengths are 2, 3.5 and 7 km, respectively. SOs generated with $\overline{\phi}$ values of 6.0° and 8.6° reach the maximum averaging length of 10 km. Additionally, one thinned raw data set is made. It is thinned to 10 km resolution in radial direction with a simple thinning algorithm which does not include any quality checks. The thinned raw data set consists of 248 000 observations, which is 27% of the original raw data.

Table 1. Summary of range bin spacing ($\overline{R}$) and azimuthal averaging ($\overline{\phi}$) parameters used in SO processing, and the corresponding number of SOs used in the experiments

	$\overline{R}$ (km)	$\overline{\phi}$ (deg)	Approx number of observations
Raw data	1	0.9	248 000 (after thinning)
SOs	5	1.7	270 000
	10	1.7	133 000
	20	1.7	77 000
	10	0.9	260 000
	10	3.4	73 000
	10	6.0	45 000
	10	8.6	33 000

3.2. HIRLAM experiment configuration

The modelled radial winds are calculated from the 6-h forecasts obtained with the hydrostatic HIRLAM model version 7.1alpha1 (Yang, 2007) with 22, 11 and 5.5 km horizontal resolutions, and with 40 vertical levels. The 22 km model run uses the ECMWF operational analyses as a lateral boundary condition. The 11 km (5.5 km) nested model run retrieves the lateral boundary conditions from the 22 km (11 km) model run. Note that the model integration areas are different in the model configurations. The forecast error of the 6-h background, and thus, the perceived observation error, is necessarily different in these configurations.

The HIRLAM 3D-Var variational data assimilation system (Gustafsson et al., 2001; Lindskog et al., 2001) is used. The resolution of the analysis is the same as the corresponding NWP model resolution. The sophisticated radar radial wind observation operator version of Part I, including modelling of the radar pulse volume broadening and the pulse path bending, is implemented in this system. In the experiments, only conventional observations of temperature, specific humidity, wind and geopotential at the pressure level of the observation site are assimilated with a 6-h cycling. The Doppler radar radial wind data are passively monitored against the modelled radial winds, i.e. no radar data are assimilated into the model.

4. Results

4.1. SO characteristics

The number of raw radial wind measurements used to form an SO (hereafter 'NUM'), and the standard deviation of the raw radial wind values forming an SO (hereafter 'SDEV') are known for each SO. Essentially, 'NUM' helps to detect SOs which contain only very few raw measurements, and 'SDEV' provides a measure for quality check purposes of the internal SO variability.

Figure 5 shows the mean, maximum and minimum values for 'NUM' as a function of measurement range for SOs generated with $\overline{\phi} = 3.4^\circ$ and $\overline{R} = 10$ km. The maximum 'NUM' increases as a function of range, as does the mean 'NUM'. The minimum 'NUM' is equal to 1 at all ranges. This indicates that these SOs represent isolated raw observations. There is a considerable possibility that such isolated observations originate from non-meteorological targets. A large value for 'NUM', on the other hand, indicates that these SOs represent more extensive areal coverage of hydrometeors. The general behaviour of the other SO data sets is similar to Fig. 5, but the maximum 'NUM' depends on $\overline{\phi}$ and $\overline{R}$.

Figure 6 shows the average 'SDEV' for different SO resolutions as a function of range. A small value for 'SDEV' indicates a good coherence of raw radial wind values within an SO. The behaviour of 'SDEV' is systematic for all SO resolutions, such that it increases with $\overline{\phi}$, and to some extent with measurement range. This implies that 'SDEV' increases also as a function of 'NUM' because the longer is the measurement range, or the wider is $\overline{\phi}$, the larger is the averaging area and consequently the larger is the average 'NUM'.

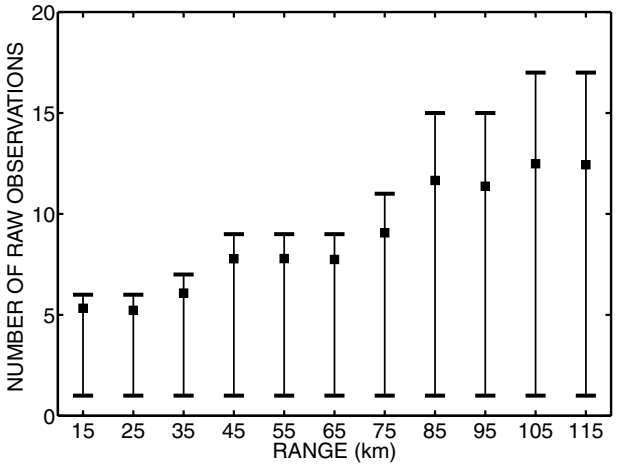

Fig. 5. Mean (black squares), maximum (upper edge of the bar) and minimum (lower edge of the bar) number of raw observations (parameter 'NUM') used in the SO processing as a function of measurement range. SOs have been generated with range bin spacing of 10 km, and azimuthal averaging 3.4°.

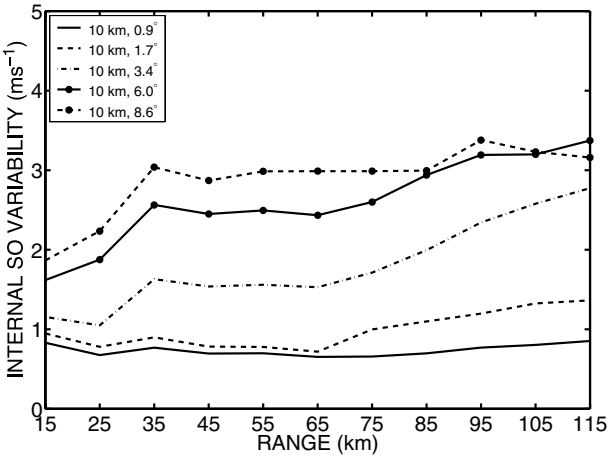

Fig. 6. Average internal SO variability (parameter 'SDEV') for different SO resolutions as a function of measurement range.

Both 'NUM' and 'SDEV' can be used as quality indicators for SOs in data screening and quality control. For example observations exceeding a pre-defined value for the internal SO variability, or observations with long measurement range and 'NUM' close to one could be rejected as suspicious. No screening or quality control is applied in this study.

4.2. Optimal SO resolution

Next, the fit of the HIRLAM model background with the radially thinned raw data and the SOs generated with varying $\overline{R}$ and $\overline{\phi}$ is studied in terms of OmB statistics. Here, the mean OmB difference for vector wind (bias) and the standard deviation of the OmB difference for radial wind component are considered. Bias estimation is done following Salonen et al. (2007). Calculating bias simply by summing up radial wind OmB values results in a near-zero bias, even in presence of systematic wind speed and/or direction differences. Random errors, in contrast, are evenly distributed in all azimuth directions and estimation of the OmB standard deviation is straightforward for the radial wind components.

First, SOs generated with varying $\overline{R}$ and a constant $\overline{\phi}$ of 1.7° are considered. The bias and the standard deviation are very large for SOs generated with $\overline{R} = 5$ km at measurement ranges shorter than 10 km (not shown). The reason for this is that at short ranges radar measurements are contaminated with ground clutter as the lower part of the radar pulse volume hits the ground, buildings etc. The SO data set where $\overline{R} = 5$ km includes notably more of these erratic measurements than the other two SO data sets. The bias and the standard deviation are on the same level for all three SO data sets, if observations from measurement ranges shorter than 10 km are excluded. Thus the choice of the parameter $\overline{R}$ is not very critical, at least not in these studied data sets, and it affects mainly the data amounts. Using $\overline{R} =$ 5 km ($\overline{R} = 20$ km) doubles (halves) the data amount compared

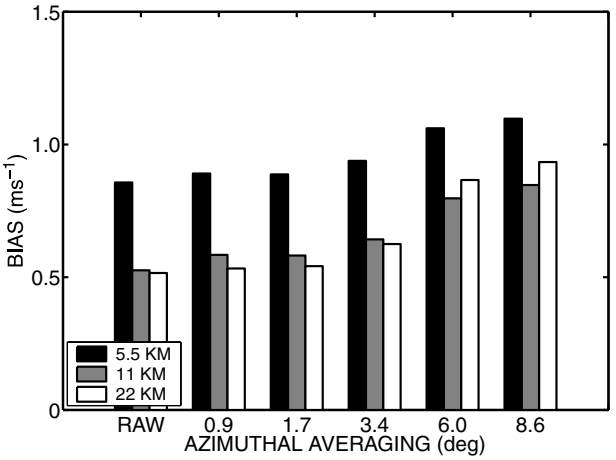

Fig. 7. Vector wind bias shown as a function of azimuthal averaging ($\overline{\phi}$) used in the SO processing. The thinned raw data are marked with 'RAW'. Black (grey, white) bars indicate 5.5 km (11 km, 22 km) NWP model resolution, respectively.

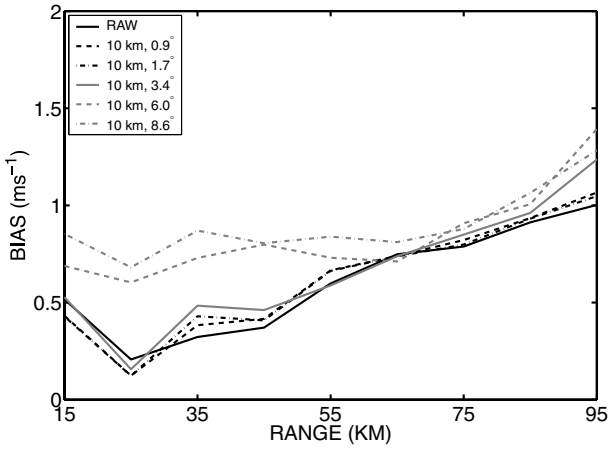

Fig. 8. Vector wind bias shown as a function of measurement range for the 11 km resolution model run. Black solid, dashed and dash–dotted lines indicate the thinned raw data and SOs with azimuthal averaging of 0.9° and 1.7°, respectively. Grey solid, dashed and dash–dotted lines indicate the SOs with azimuthal averaging of 3.4°, 6.0° and 8.6°, respectively.

to using $\overline{R}$ =10 km. In the following, $\overline{R}$ is kept constant at 10 km. The choice is justified as the data sets are large enough for reliable bias estimation and the data handling is convenient.

Next, varying $\overline{\phi}$ is considered. Figure 7 illustrates the OmB vector wind bias as a function of $\overline{\phi}$. The radially thinned raw data set is marked with 'RAW'. The vector wind bias is the smallest for the thinned raw data set. Among the SO data sets, bias increases with $\overline{\phi}$. This is the case for all NWP model resolutions. Different magnitudes of the bias for different NWP model resolutions is a direct consequence of the different model errors in these model configurations.

The vector wind bias consists of wind speed and wind direction biases. The wind speed bias is the smallest for the thinned raw data set and it increases systematically with $\overline{\phi}$ (not shown). The wind speed bias is negative (modelled wind is stronger than the observed one). The wind direction bias is less than 1.5° for all data sets, i.e. it is relatively small (not shown). In the studied data sets, the vector wind bias is dominated by the wind speed bias rather than the wind direction bias. The vector wind bias is thus the smallest for the radially thinned raw data set.

Figure 8 displays the vector wind bias for different data sets as a function of range for the 11 km NWP model resolution. Black solid, dashed and dash–dotted lines indicate the thinned raw data set and the SO data sets with $\overline{\phi}$ equal to 0.9° and 1.7°, respectively. Grey solid, dashed and dash–dotted lines indicate the SO data sets with $\overline{\phi}$ equal to 3.4°, 6.0° and 8.6°, respectively. The bias generally increases with $\overline{\phi}$. Differences in the vector wind bias between different data sets are the largest at 25 km range, and they become somewhat smaller at longer ranges. The smallest bias at measurement ranges below 35 km is for the SO data set with $\overline{\phi} = 0.9°$. At longer ranges, the thinned raw data have the smallest bias. In this sense, Fig. 8 is consistent with Fig. 7 where the smallest vector wind bias is found for the thinned raw measurements. The vector wind bias for 5.5 and 22 km NWP model resolutions (not shown) is very similar as for the 11 km resolution. In conclusion, the smallest bias is obtained for the thinned raw data or for the SO data set with $\overline{\phi} = 0.9°$, depending on the range, and the largest for the SO data sets with $\overline{\phi} = 6.0°$ or $\overline{\phi} = 8.6°$.

The increase in the wind speed bias as a function of range can be explained by the fact that the radar pulse volume broadens with increasing range and the probability for overshooting increases, i.e. the pulse volume may be partly, or even mainly, above the scatterers. In such cases, the measurement originates from the lower part of the pulse volume and the actual measurement height is lower than the modelled one. The hypothesis has been validated by studying the SOs originating from different elevation angles separately (not shown). For measurement ranges longer than 75 km, the bias is indeed the smallest for the lowest elevation angle (0.5° in these data sets) and the magnitude of the bias increases systematically as the elevation angle increases. Clearly, for high elevation angles, the radar pulse volume overshooting occurs on average at shorter ranges.

Increasing wind speed bias as a function of $\overline{\phi}$ may be partly explained by the fact that using a wide $\overline{\phi}$ in the SO processing reduces the maximum (towards and away from the radar antenna) wind speeds. However, as discussed in Section 2.2, in simplified cases of uniform and linear wind fields, this artificial bias is extremely small. Figure 8 reveals that the differences in the vector wind bias for different data sets are the largest at short measurement ranges. This evokes an idea that the raw data set from which the SOs have been generated may contain ground clutter or other non-meteorological observations, even though clutter removal has been performed prior the SO generation. The increase in the bias as a function of azimuthal averaging

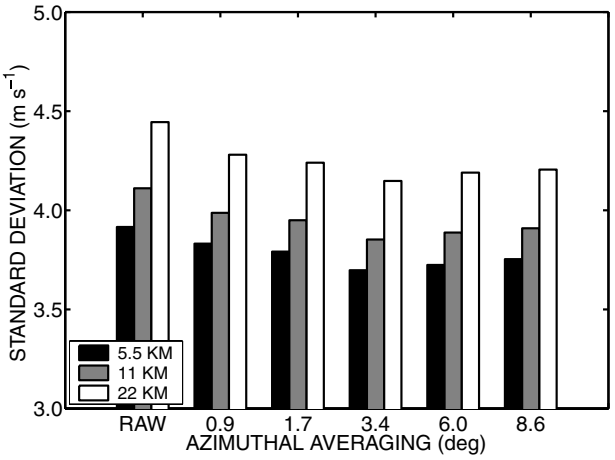

Fig. 9. As Fig. 7 but for the standard deviation of radar radial wind component.

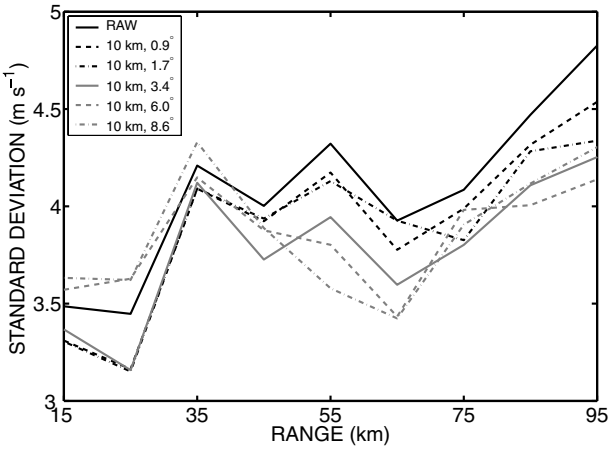

Fig. 10. As Fig. 8 but for the standard deviation of radar radial wind component.

is significantly stronger if ground clutter is present in the data as illustrated in Section 2.2. Thus, the increase of the bias as a function of $\overline{\phi}$ seen in Figs. 7 and 8 may be a consequence of remaining clutter in the raw data.

Figure 9 displays OmB standard deviation of radial wind components as a function of $\overline{\phi}$. The OmB standard deviation decreases until it reaches the minimum at SOs generated with $\overline{\phi} = 3.4^\circ$, and increases again for wider $\overline{\phi}$. The OmB standard deviation behaves similarly in all three considered NWP model resolutions. This implies that processing SOs with an increasing azimuthal averaging distance decreases random errors up to a certain limit, here $\overline{\phi} = 3.4^\circ$. However, too wide $\overline{\phi}$ degrades the SO quality.

Finally, the OmB standard deviation of radial wind component is shown as a function of range (Fig. 10) for the 11 km NWP model resolution. The OmB standard deviation varies between 3.2 and 4.8 ms^{-1} and it generally increases as a function of measurement range. Standard deviation for the thinned raw data is large, except at short measurement ranges. Processing SOs improves the OmB standard deviation statistics over the thinned raw measurements. Almost any value for $\overline{\phi}$ would do: most beneficial is $\overline{\phi} = 0.9^\circ$–$3.4^\circ$ at short ranges (below 35 km), while at longer ranges (above 35 km) it is $\overline{\phi} = 3.4^\circ$–$8.6^\circ$. The OmB standard deviations for NWP model resolutions 5.5 and 22 km are very similar (not shown). It is concluded that random errors can be partly eliminated by the SO processing.

4.3. Recommendations for the SO processing parameters

In conclusion, a set of HIRLAM model experiments has been performed to define optimal values for the free parameters in the SO processing, namely range bin spacing $\overline{R}$ and azimuthal averaging $\overline{\phi}$. The HIRLAM NWP model horizontal resolutions of 5.5, 11 and 22 km have been studied.

Results from the experiments with $\overline{R} = 5$–20 km and a constant $\overline{\phi} = 1.7^\circ$ reveal that the data set with $\overline{R} = 5$ km includes a lot of erratic data with measurement ranges shorter than 10 km. If observations from those measurement ranges are excluded, all three SO data sets behave very similarly. Thus, the choice of the value for $\overline{R}$ is not as critical as the choice of $\overline{\phi}$ in the SO processing. A constant value of 10 km has been adopted here for two reasons. First, data sets with $\overline{R} = 10$ km are large enough for reliable bias estimation, unlike the data sets with $\overline{R} = 20$ km and wide values for $\overline{\phi}$. Second, being only half the size of the data sets with $\overline{R} = 5$ km makes the data handling easier.

Results from the model experiments with varying $\overline{\phi}$ indicate that the vector wind bias is the smallest for the radially thinned raw observations, and it increases with increasing $\overline{\phi}$. However, the increase in the bias for SOs with $\overline{\phi}$ equal to 0.9° and 1.7° is relatively small compared to the bias in the thinned raw data. All NWP model resolutions behave similarly. Thus, using a wide $\overline{\phi}$ in the SO processing degrades the SO quality in terms of increasing bias. The use of thinned raw data would be recommended if the choice of $\overline{\phi}$ is made only based on bias.

The impact of random errors can be, to some extent, decreased by the SO processing. In these experiments, the OmB standard deviation is the largest for the thinned raw data and it decreases until it reaches the minimum with $\overline{\phi} = 3.4^\circ$. This corresponds to averaging raw observations from four adjacent azimuth angles. For wider $\overline{\phi}$, the standard deviation begins to increase again. SOs generated with $\overline{\phi} = 3.4^\circ$ would be recommended if the choice of $\overline{\phi}$ is made only based on standard deviation.

For user applications, a balance between the vector wind bias and the radial wind standard deviation is obtained by setting $\overline{\phi}$ equal to 0.9° or 1.7°. Additionally, data amount can be used as a secondary optimality criterion. If a large (small) data volume is preferred, $\overline{\phi} = 0.9^\circ (\overline{\phi} = 1.7^\circ)$ is recommended.

The SO processing algorithm adopted in the HIRLAM framework is specific with its free parameters $\overline{R}$ and $\overline{\phi}$. In more

general terms, the parameter value $\overline{\phi} = 1.7^\circ$ correspond at 50 km (100 km) measurement range a 1.7 km^2 (7.3 km^2) averaging area.

5. Summary

The HIRLAM 3D-Var data assimilation system has been further developed to include the capability of assimilating Doppler radar radial wind observations. The observation modelling is considered in Part I of this article. Part II concentrates on optimizing the SO processing for varying NWP model resolutions. It is shown that the impact of random observation errors of the radial winds can be decreased by SO processing from the raw observations.

The HIRLAM approach to the radial wind SO processing is based on spatial averaging in polar space. The averaging area is defined by two free parameters, range bin spacing and azimuthal averaging. In the chosen strategy, averaging area increases as a function of measurement range. Thus, fewer raw observations influence an SO near the radar than at longer measurement ranges. Averaging of raw observations with significantly different azimuth directions introduces artificial bias and should be avoided.

Experiments with the HIRLAM model horizontal resolutions of 5.5, 11 and 22 km, and with eight SO data sets with different resolutions, including a set of radially thinned raw observations, have been used to determine optimal values for the SO processing parameters. Observation minus background statistics indicate that the mean vector wind OmB difference is the smallest for the thinned raw data, while the smallest OmB standard deviation of the radial wind speed is obtained by processing SOs from raw measurements. It appears that varying the azimuthal averaging is more critical than varying the range bin spacing. Values of 0.9° or 1.7° for the azimuthal averaging are recommended here. At 50 km (100 km) range $\overline{\phi} = 1.7^\circ$ implies an averaging area of 1.7 km^2 (7.3 km^2).

6. Acknowledgments

The research has been funded by the Academy of Finland project 'Doppler radar wind data assimilation' in 2002–2005 and its continuation in 2006. We acknowledge Daniel Michelson from the Swedish Meteorological and Hydrological Institute (SMHI) for providing the RAVE software. The anonymous peer-reviewers are gratefully acknowledged for the constructive comments.

References

Albers, S. 1995. The LAPS wind analysis. *Wea. Forecast.* **10**, 342–352.

Berger, H., Forsythe, M., Eyre, J. and Healy, S. 2004. *Proceedings of the seventh international winds workshop*, Helsinki, Finland, EUM P.42, 119–126. Available at www.eumetsat.int/Home/Main/Publications/

Daley, R. 1991. *Atmospheric Data Analysis*. Cambridge University Press, United Kingdom, 457 pp.

Dazhang, T., Geotis, S. G., Passarelli, R. E. Jr., Hansen, A. L. and Frush, C. L. 1984. Evaluation of an alternating-PRF method for extending the range of unambiguous Doppler velocity. In: *Proceedings of 22d Conf. on Radar Meteorology,* Zurich, Switzerland, Am. Meteorol. Soc. (preprints), 523–527.

Gustafsson, N., Berre, L., Hörnquist, S., Huang, X.-Y., Lindskog, M. and co-authors. 2001. Three-dimensional variational data assimilation for a limited area model, part I: general formulation and the background error constraint. *Tellus* **53A**, 425–446.

Hart, T., Bourke, W., Steinle, P. and Seaman, R. 1993. Impact of higher-resolution satellite soundings of temperature and moisture on large-scale numerical weather prediction. *Mon. Wea. Rev.* **121**, 1746–1758.

Holleman, I. and Beekhuis, H. 2003. Analysis and correction of dual PRF velocity data. *J. Atmos. Ocean. Technol.* **20**, 443–453.

Kalnay, E. 2003. *Atmospheric Modeling, Data Assimilation and Predictability*. Cambridge University Press, United Kingdom, 341 pp.

Lindskog, M., Järvinen, H. and Michelson, D. B. 2000. Assimilation of radar radial winds in the HIRLAM 3D-Var. *Phys. Chem. Earth (B)* **25**, 1243–1249.

Lindskog, M., Gustafsson, N., Navascués, B., Mogensen, K. S., Huang, X.-Y. and co-authors. 2001. Three-dimensional variational data assimilation for a limited area model, part II: observation handling and assimilation experiments. *Tellus* **53**, 447–468.

Lindskog, M., Salonen, K., Järvinen, H. and Michelson, D. B. 2004. Doppler radar wind data assimilation with HIRLAM 3DVAR. *Mon. Wea. Rev.* **132**, 1081–1092.

Liu, Z. Q. and Rabier, F. 2003. The potential of high-density observations for numerical weather prediction: a study with simulated observations. *Quart. J. R. Meteorol. Soc.* **129**, 3013–3035.

Lorenc, A. C. 1981. A global three dimensional multivariate statistical interpolation scheme. *Mon. Wea. Rev.* **109**, 701–721.

Lorenc, A. C. 1986. Analysis methods for numerical weather prediction. *Quart. J. R. Meteorol. Soc.* **112**, 1177–1194.

Lönnberg, P. and Shaw, D. 1983. Research manual 1. ECMWF data assimilation. Scientific documentation. 103 pp.

Salonen, K., Järvinen, H., Eresmaa, R. and Niemelä, S. 2007. Bias estimation of Doppler-radar radial-wind observations. *Quart. J. R. Meteorol. Soc.* **133**, 1501–1507.

Seko, H., Kawabata, T., Tsuyuki, T., Nakamura, H., Koizumi, K. and co-authors. 2004. Impacts of GPS-derived water vapor and radial wind measured by Doppler radar on numerical prediction of precipitation. *J. Meteorol. Soc. Jpn.* **82**, 473–489.

Swarbrick, S. 2006. Assimilation of Doppler radar radial winds. In: *Proceedings of the Fourth European Conference on Radar Meteorology and Hydrology*, Barcelona, Spain, 527–530.

Undén, P., Rontu, L., Järvinen, H., Lynch, P., Calvo, J. and co-authors. 2002. HIRLAM-5 Scientific Documentation, SMHI, Norrköping, Sweden, 144 pp.

Xiao, Q., Sun, J., Lee, W., Lim, E., Guo, Y. and co-authors. 2003. Assimilation of Doppler radar observations with a regional 3D-Var system: a heavy rainfall case study. In: 31st Conf. on Radar Meteorology *Proceedings of 31st Conf. on Radar Meteorology* Volume 1, Seattle, WA, Am. Meteorol. Soc. (preprints), 165–168.

Yang, X. 2007. Status of the HIRLAM reference system. *HIRLAM Newslett.* **52**, 172–175. KNMI, De Bilt, The Netherlands. Available at http://hirlam.org/open/publications/NewsLetters.